

Size controlled synthesis of uniform $\text{Li}_2\text{MnSiO}_4$ nanospheres and their electrochemical behaviors in lithium-ion batteries

Xiangzhi Kong¹, Tao Mei¹, Zheng Xing¹, Na Li¹, Zhengqiu Yuan¹, Yongchun Zhu^{1,*} and Yitai Qian^{1,2,*}

¹ Hefei National Laboratory for Physical Science at Microscale and Department of Chemistry, University of Science and Technology of China, Hefei, Anhui 230026, P.R. China

² School of Chemistry and Chemical Engineering, Shandong University, Jinan 250100, P.R. China

*E-mail: ytqian@ustc.edu.cn

Received: 16 April 2012 / Accepted: 14 May 2012 / Published: 1 June 2012

The uniform $\text{Li}_2\text{MnSiO}_4$ nanospheres with diameters of ~500 and 300 nm have been selectively prepared via monodisperse spherical SiO_2 precursors with corresponding sizes by solid state method. Furthermore, $\text{Li}_2\text{MnSiO}_4/\text{C}$ composites were obtained by annealing $\text{Li}_2\text{MnSiO}_4$ nanospheres with glucose at 400 °C. Electrochemical measurements show that spherical $\text{Li}_2\text{MnSiO}_4/\text{C}$ with a diameter of ~300 nm exhibits first discharge capacity of 145 mAh g⁻¹, together with a stable discharge capacity of 121 mAh g⁻¹ after 50 cycles, which are higher than that with a diameter of ~500 nm.

Keywords: $\text{Li}_2\text{MnSiO}_4$; Nanospheres; SiO_2 ; Size control; Lithium-ion batteries

1. INTRODUCTION

The orthosilicates, Li_2MSiO_4 (where M = Mn^{2+} , Fe^{2+} , Co^{2+} , Ni^{2+}) [1-8], have been recognized as one of the most promising candidates in lithium-ion batteries (LIBs) due to its low cost, high safety, structure stability, and environmental friendliness. The most attractive feature is that Li_2MSiO_4 have a high theoretical capacity of 333 mAh g⁻¹ by the insertion/extraction of two lithium ions per formula unit.

Since Dominko et al. [9] first reported the synthesis and electrochemical performance of $\text{Li}_2\text{MnSiO}_4$, considerable research efforts have been directed to design and synthesis of $\text{Li}_2\text{MnSiO}_4$ with enhanced electrochemical performance. Various methods have been developed to prepare $\text{Li}_2\text{MnSiO}_4$, mainly including sol gel method [10], solid state reaction [11], and hydrothermal process [12]. For instance, $\text{Li}_2\text{MnSiO}_4$ was prepared by an all-acetate sol gel method using tetraethyl orthosilicate (TEOS) as silicon source which showed large aggregates (10-50 μm) composed of

nanosized particles (100-200 nm). The as-obtained products presented a discharge capacity of 98 mAh g⁻¹ after 15 cycles under 10 mA g⁻¹ [13]. Aravindan et al. prepared Li₂MnSiO₄ by solid state method using SiO₂ as silicon source, and irregular particulate morphology with some sort of aggregation was observed. When the carbon contents were 42 and 12%, discharge capacities of 140 and 25 mAh g⁻¹ after 40 cycles at 0.05 C were obtained, respectively [14].

As we known that the electrochemical performance of materials depends significantly on the particle size, so it is important to control the particle size and study its effects on cell performance [15]. While some groups have reported the synthesis of nanocrystalline Li₂MnSiO₄, size controlled synthesis of Li₂MnSiO₄ and investigation of the relationship between electrochemical performance and the particle size have been less carried out due to the difficulties in controlling the particle size. In particular, tailoring the particle morphology and size in solid state synthesis is more complicated than other methods because of the experiment being conducted at high temperature, which may usually results in irregular particulate morphology and strongly aggregation.

Herein, we have devised a size controlled synthesis of uniform Li₂MnSiO₄ nanospheres by solid state method, where monodisperse SiO₂ spheres with different sizes were used as precursors. Li₂MnSiO₄ nanospheres with diameters of ~500 and 300 nm have been prepared successfully. Li₂MnSiO₄ nanospheres were coated by carbon layers using glucose as carbon source to improve the low inherent electronic conductivity. The influence of particles size on electrochemical performance of Li₂MnSiO₄/C has been studied, which shows that spherical Li₂MnSiO₄/C with a diameter of ~300 nm displays higher reversible capacity and better cycle stability than that with a diameter of ~500 nm.

2. EXPERIMENTAL

All the chemical reagents used here were analytical grade, and were used without further purification.

2.1 Synthesis of SiO₂ spheres

Monodisperse SiO₂ solid spheres with diameters of ~500 and 300 nm were performed by a slightly modified Stöber process [16,17].

Synthesis of ~500 nm SiO₂ spheres: 4.5 mL of TEOS was rapidly added into the mixture of 9 mL of ammonium hydroxide (28%), 24.75 mL of distilled water and 61.75 mL of absolute ethanol under stirring and kept for 3 h. The white precipitates were centrifuged and washed with absolute ethanol several times. The products were dried in a vacuum at 60 °C for 3 h.

Synthesis of ~300 nm SiO₂ spheres: 0.6 mL of TEOS, 0.7 mL of ammonium hydroxide (28%), 5 mL of distilled water and 15 mL absolute ethanol were used. The experimental procedures were the same as those described above.

2.2 Synthesis of $\text{Li}_2\text{MnSiO}_4$ and $\text{Li}_2\text{MnSiO}_4/\text{C}$ nanospheres

Stoichiometric amount of $\text{LiOH}\cdot\text{H}_2\text{O}$, SiO_2 (as-prepared), MnCO_3 were finely ground using mortar and pestle and fired at $400\text{ }^\circ\text{C}$ for 4 h in air. Then the intermediate products were ground and then calcined at $700\text{ }^\circ\text{C}$ for 12 h in flowing argon (5wt%, H_2). The as-prepared samples were labeled as Sample 1 (~500 nm in diameter) and Sample 2 (~300 nm in diameter) respectively.

The as-prepared Sample 1 and Sample 2 were mixed with 40wt% glucose and carbonized at $400\text{ }^\circ\text{C}$ for 4 h under Ar (5wt%, H_2) flow to obtain $\text{Li}_2\text{MnSiO}_4/\text{C}$ composites and were labeled as Sample 3 and Sample 4, respectively.

2.3 Materials characterization

X-ray powder diffraction (XRD) patterns of the products were recorded on a Philips X'pert X-ray diffractometer with $\text{Cu K}\alpha$ radiation ($\lambda=1.54182\text{ \AA}$). The microstructure was observed with a field-emitting scanning electron microscope (SEM, JEOL-JSM-6700F), a transmission electron microscope (TEM, H7650), and a high-resolution transmission electron microscope (HRTEM, JEOL-2010) with an accelerating voltage of 200 kV. Raman spectrums were carried out on a JY LABRAM-HR confocal laser micro-Raman spectrometer using Ar^+ laser excitation with a wavelength of 514.5 nm. X-ray Photoelectron Spectrum measurements (XPS) were performed by using a VGESCA-LABMKIIX-ray photoelectron spectrometer. Elemental analyses were carried out on a vario EL-III elemental analyzer (Germany).

2.4 Electrochemical measurements

Charge/discharge tests were carried out using CR 2016 coin-type cells. The active material, acetylene black and polyvinylidene fluoride (PVDF) with a weight ratio of 70:20:10 were mixed homogeneously with N-methyl-pyrrolidone, the obtained slurry was pasted on Al foil and dried at $100\text{ }^\circ\text{C}$ for 12 h in vacuum. The electrode sheet typically had an active material of $\sim 1\text{ mg cm}^{-2}$. The coin cell was then assembled in an argon-filled glove box (Mikrouna, Super 1220/750/900, China) and consisted of $\text{Li}_2\text{MnSiO}_4$ (cathode), Celgard 2400 (separator), and lithium foil (anode). 1 mol L^{-1} solution of LiPF_6 dissolved in ethylene carbonate/dimethyl carbonate (EC/DMC) (1:1 volume ratio) was used as the electrolyte. Galvanostatic charge/discharge measurements were performed in a potential range of 1.5-4.8 V at room temperature on a LAND-CT2001A instrument.

3. RESULTS AND DISCUSSION

Fig. 1 shows the XRD patterns of as-synthesized $\text{Li}_2\text{MnSiO}_4$ (Sample 1, 2) and $\text{Li}_2\text{MnSiO}_4/\text{C}$ (Sample 3, 4). All patterns have similar diffractions without obvious difference. The crystalline peaks can be identified as orthorhombic $\text{Li}_2\text{MnSiO}_4$ with a space group of $\text{Pmn}2_1$ which is isostructural to the low-temperature $\beta\text{-Li}_3\text{PO}_4$, The calculated cell parameters for this material are $a = 6.2991\text{ \AA}$, $b =$

5.3794 Å and $c = 5.0009$ Å, which are in good agreement with values published by previous literatures [9]. Additional peaks are observed in the diffractograms, which have been identified as MnO.

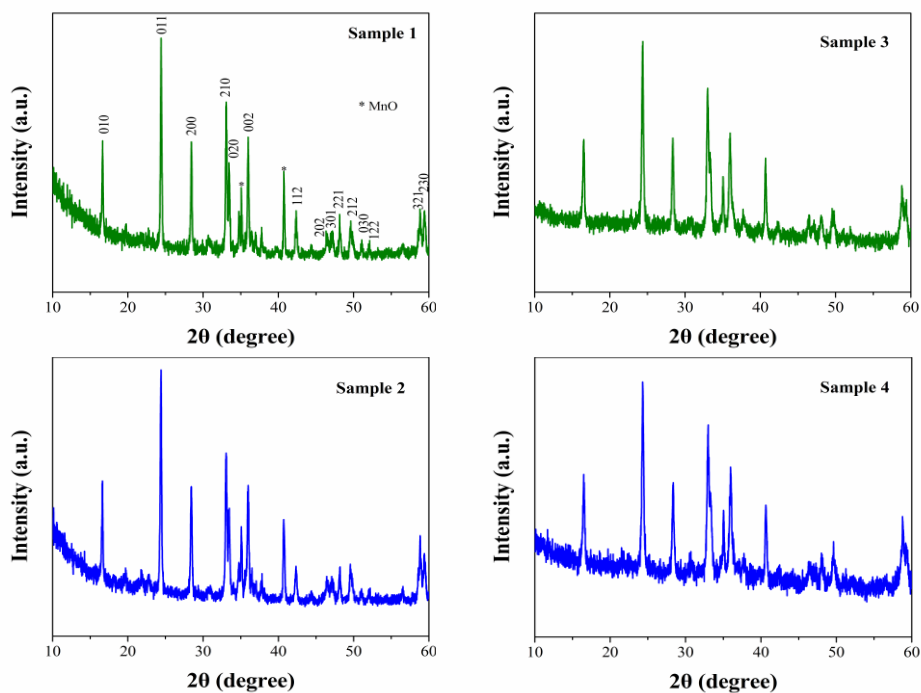


Figure 1. XRD patterns of as-prepared $\text{Li}_2\text{MnSiO}_4$ (Sample 1, 2) and $\text{Li}_2\text{MnSiO}_4/\text{C}$ (Sample3, 4).

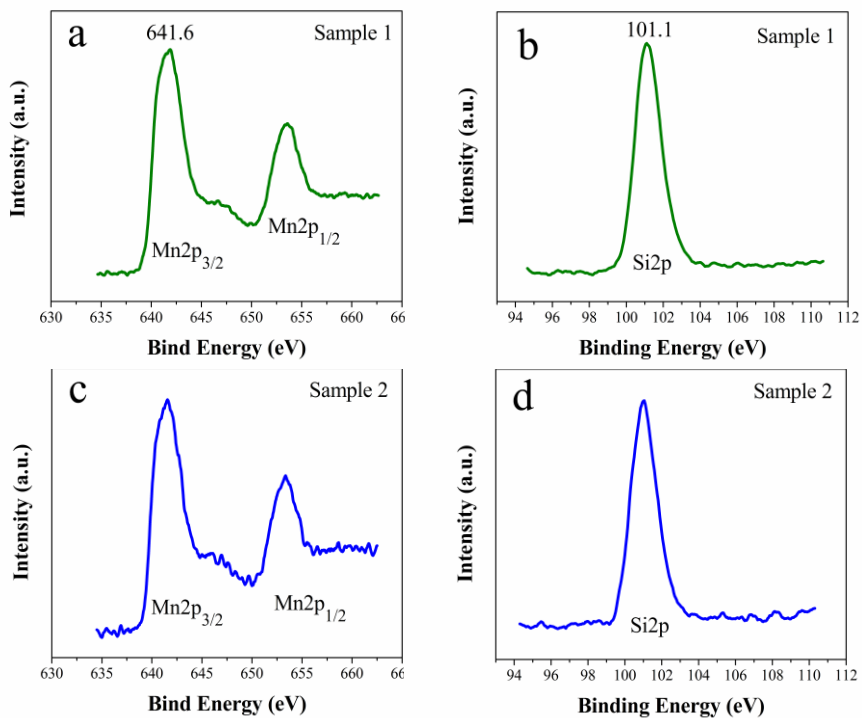


Figure 2. XPS spectra of Sample 1 and Sample 2: (a, c) Mn 2p and (b, d) Si 2p.

Obtaining a phase pure $\text{Li}_2\text{MnSiO}_4$ material by solid state method is still a challenge, the impurities phases like Li_2SiO_3 , MnO or Mn_2SiO_4 are also present in previous reports [6,11]. XRD patterns of Sample 3 and Sample 4 indicate that there are no peaks for carbon which could attribute to the amorphous nature or low quantity of carbon. The carbon contents in Sample 3 and Sample 4 were determined to be about 15.18 and 14.96wt% respectively by elementary analysis.

The Mn 2p and Si 2p XPS spectra of Sample 1 and Sample 2 are shown in Fig. 2. The binding energy of Mn 2p_{3/2} (641.6 eV) is consistent with that of Mn^{2+} , indicating that the divalent state of manganese in our samples. The binding energy of Si 2p (101.1 eV) is in line with that of Si^{4+} in polysiloxane, indicating the formation of the orthosilicate structure $[\text{SiO}_4]$ [18].

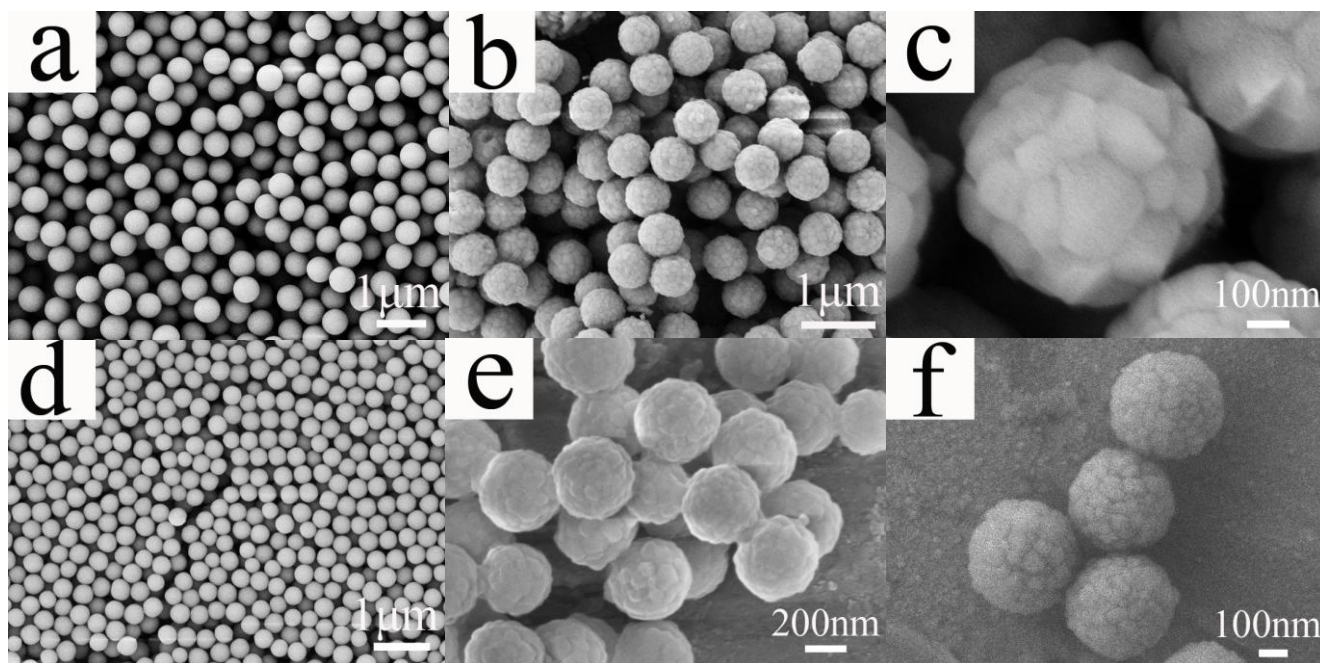


Figure 3. Typical SEM images of (b, c) Sample 1, (e, f) Sample 2 and corresponding monodisperse spherical SiO_2 precursors with a size of about (a) 500 nm, (d) 300 nm.

SEM images of Sample 1 and Sample 2 and corresponding SiO_2 precursors are shown in Fig. 3. All the samples clearly exhibit uniform sphere-like morphology. Fig. 3a, d show typical SEM images of monodisperse SiO_2 solid spheres of about 500 and 300 nm respectively in diameter prepared by the well-known Stöber process. Sample 1 and Sample 2 exhibit uniform nanosphere-like morphology with diameters of ~500 and 300 nm respectively (Fig. 3b, e). The particle sizes in Fig. 3b, e are very similar to Figure 3a, d respectively which indicate that $\text{Li}_2\text{MnSiO}_4$ approximately retains the uniform spherical morphology and size of corresponding SiO_2 precursor. The magnified SEM images in Fig. 3c, f clearly show that the surfaces of the nanospheres are not smooth and may be result of an agglomeration of $\text{Li}_2\text{MnSiO}_4$ grains. SEM images demonstrate that the particle size of $\text{Li}_2\text{MnSiO}_4$ is successfully controlled by regulating the size of SiO_2 precursors, which providing the possibility of size controlled synthesis of uniform spherical $\text{Li}_2\text{MnSiO}_4$ by a traditional solid state method.

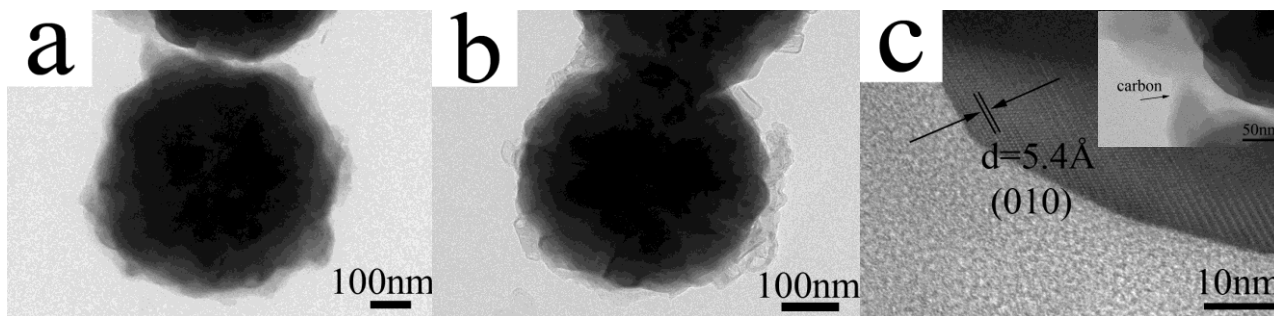


Figure 4. TEM images of (a) Sample 3, (b) Sample 4, and (c) HRTEM images of Sample 3.

$\text{Li}_2\text{MnSiO}_4/\text{C}$ composites were observed by TEM and HRTEM. Fig. 4a, b show the TEM images of Sample 3 and Sample 4, in which the core-shell structure could be observed. $\text{Li}_2\text{MnSiO}_4$ nanospheres are uniformly coated by carbon layers. The HRTEM image of Sample 3 (inset of Fig. 4c) further confirm that the structure are constructed by $\text{Li}_2\text{MnSiO}_4$ core and carbon shell. The strong contrast between the light edge and dark center of the composite provide evidence of its core-shell structure. Crystal lattice stripes of Sample 3 (Fig. 4c) are observed with d-spacing of 5.4 Å, which corresponds to the (010) plane of orthorhombic $\text{Li}_2\text{MnSiO}_4$ crystals.

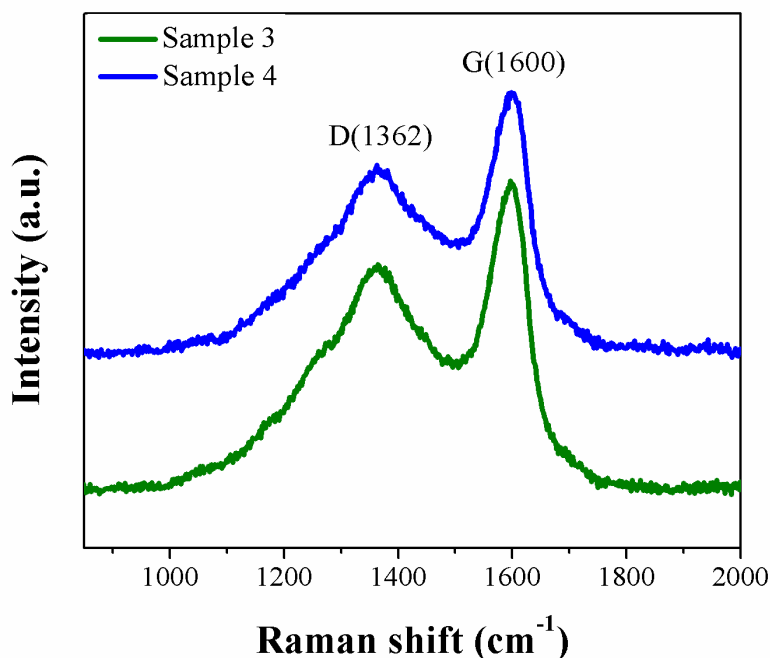


Figure 5. Raman spectra of Sample 3 and Sample 4.

Raman spectroscopy has emerged in recent years as powerful tool to examine the carbon component of nanocomposites. Fig. 5 shows the Raman spectra of Sample 3 and Sample 4

respectively. The D band (1362 cm^{-1}) comes from disordered carbon, while the G band (1600 cm^{-1}) is related to the graphite. The I_D/I_G ratios of Sample 3 and Sample 4 are found to be 1.87 and 1.79 respectively, demonstrating that a mass of the coated carbon is fairly amorphous. The Raman datas agree with the HRTEM images and XRD patterns.

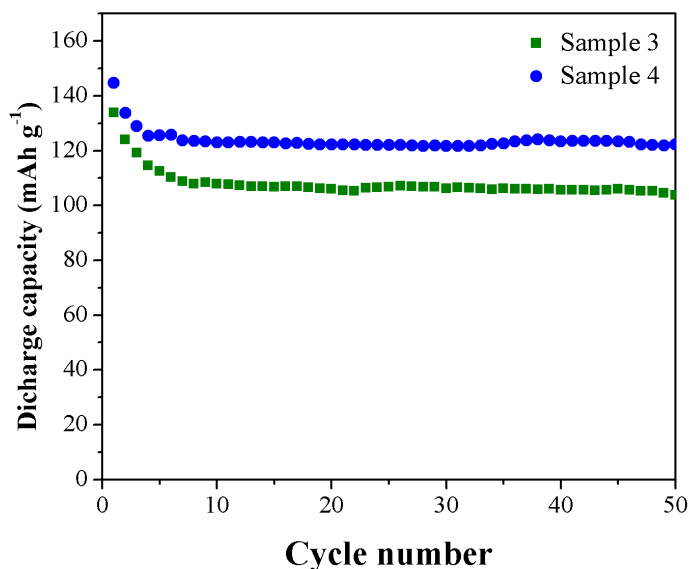


Figure 6. The cycling performances of Sample 3 and Sample 4 measured at 0.05 C in room temperature.

The electrochemical performances of as-prepared $\text{Li}_2\text{MnSiO}_4/\text{C}$ nanospheres were investigated. Fig. 6c shows the discharge capacities and cyclic performances of Sample 3 and Sample 4 at 0.05 C in room temperature. In the voltage range of 1.5–4.8 V, the initial discharge capacities of the samples are 134 and 145 mAh g^{-1} respectively. The capacities fade fast at first, and keep stable after 5 cycles. After 50 cycles, the capacities retentions of the samples are 99 and 121 mAh g^{-1} , corresponding to 74 and 83% of those in the initial cycle respectively, which demonstrate stable cycle behavior. This result suggests that $\text{Li}_2\text{MnSiO}_4/\text{C}$ nanospheres with a diameter of $\sim 300\text{ nm}$ display higher discharge capacity and better cycle stability than that with a diameter of $\sim 500\text{ nm}$. The reasons could attribute to the materials with smaller size providing short pathways for quick lithium ion, electronic conduction within the nanoparticles and larger surface area for contracting with electrolyte, which can improve the rate capability and cycling stability of materials [12].

Although nanostructuring is expected to improve the electrochemical performance of $\text{Li}_2\text{MnSiO}_4$, very small particles often do not pack well resulting in lower practical volume energy densities [19]. In addition, when used as electrode materials, spherical particles can allow for a denser packing, showing an advantage of high volumetric energy density, and high safety associated with low interfacial energy [20], and it is easier to coat due to good fluidity and dispersivity of spheres. So the spherical $\text{Li}_2\text{MnSiO}_4$ is an important direction for $\text{Li}_2\text{MnSiO}_4$ cathode materials. As a whole, we

conclude that the $\text{Li}_2\text{MnSiO}_4$ electrode material which consist of large spherical agglomerates of nanosized primary particles may exhibit both enhanced electrochemical performance and volume energy density [21]. Further studies on optimizing the size and spherical morphology of $\text{Li}_2\text{MnSiO}_4$ are in progress.

4. CONCLUSIONS

Monodisperse spherical SiO_2 precursors with different sizes were used to control the size of $\text{Li}_2\text{MnSiO}_4$. $\text{Li}_2\text{MnSiO}_4$ nanospheres with diameters of ~500 and 300 nm have been successfully synthesized by a solid state method. SEM images exhibit that $\text{Li}_2\text{MnSiO}_4$ approximately retains the uniform spherul morphology and size of corresponding SiO_2 precursor. $\text{Li}_2\text{MnSiO}_4$ nanospheres were annealed with glucose at 400 °C to prepare the $\text{Li}_2\text{MnSiO}_4/\text{C}$ composites. Electrochemical measurements show that $\text{Li}_2\text{MnSiO}_4/\text{C}$ nanospheres with a diameter of ~300 nm display higher discharge capacity and better cycle stability than that with a diameter of ~500 nm.

In this paper, we provide an effective method to prepare $\text{Li}_2\text{MnSiO}_4$ products with regular spherical morphology and different particle sizes. It is notable that various morphologies and sizes of SiO_2 have been studied in a mass of reports [16,22,23]. $\text{Li}_2\text{MnSiO}_4$ with more morphologies and sizes can be expected, such as hollow spheres and nanowires et al.

ACKNOWLEDGEMENTS

This work was financially supported by the National Natural Science Fund of China (No. 91022033), the 973 Project of China (No. 2011CB935901)

References

1. A. Nyten, A. Abouimrane, M. Armand, T. Gustafsson and J. O. Thomas, *Electrochem. Commun.*, 7 (2005) 156-160
2. R. Dominko, M. Bele, A. Kokalj, M. Gaberscek and J. Jamnik, *J. Power Sources*, 174 (2007) 457-461
3. C. Lyness, B. Delobel, A. R. Armstrong and P. G. Bruce, *Chem. Commun.*, (2007) 4890-4892
4. Z. L. Gong, Y. X. Li, G. N. He, J. Li and Y. Yang, *Electrochem. Solid St.*, 11 (2008) A60-A63
5. N. Kuganathan and M. S. Islam, *Chem. Mater.*, 21 (2009) 5196-5202
6. W. G. Liu, Y. H. Xu and R. Yang, *J. Alloy Compd.*, 480 (2009) L1-L4
7. C. Sirisopanaporn, C. Masquelier, P. G. Bruce, A. R. Armstrong and R. Dominko, *J. Am. Chem. Soc.*, 133 (2011) 1263-1265
8. K. D. M. Dinesh Rangappa, *Nano. Lett.*, 12 (2012) 1146-1151
9. R. Dominko, M. Bele, M. Gaberscek, A. Meden, M. Remskar and J. Jamnik, *Electrochem. Commun.*, 8 (2006) 217-222
10. C. Deng, S. Zhang, B. L. Fu, S. Y. Yang and L. Ma, *Mater. Chem. Phys.*, 120 (2010) 14-17
11. K. Karthikeyan, V. Aravindan, S. B. Lee, I. C. Jang, H. H. Lim, G. J. Park, M. Yoshio and Y. S. Lee, *J. Power Sources*, 195 (2010) 3761-3764
12. T. Muraliganth, K. R. Stroukoff and A. Manthiram, *Chem. Mater.*, 22 (2010) 5754-5761
13. I. Belharouak, A. Abouimrane and K. Amine, *J. Phys. Chem. C*, 113 (2009) 20733-20737

14. V. Aravindan, K. Karthikeyan, K. S. Kang, W. S. Yoon, W. S. Kim and Y. S. Lee, *J. Mater. Chem.*, 21 (2011) 2470-2475
15. S. H. Choi, J. W. Son, Y. S. Yoon and J. Kim, *J. Power Sources*, 158 (2006) 1419-1424
16. T. Zhang, Q. Zhang, J. Ge, J. Goebel, M. Sun, Y. Yan, Y. Liu, C. Chang, J. Guo and Y. Yin, *J. Phys. Chem. C*, 113 (2009) 3168-3175
17. Q. Yu, P. Wang, S. Hu, J. Hui, J. Zhuang and X. Wang, *Langmuir*, 27 (2011) 7185-7191
18. Y. X. Li, Z. L. Gong and Y. Yang, *J. Power Sources*, 174 (2007) 528-532
19. J. Liu, T. E. Conry, X. Y. Song, L. Yang, M. M. Doeff and T. J. Richardson, *J. Mater. Chem.*, 21 (2011) 9984-9987
20. J. Ying, C. Jiang and C. Wan, *J. Power Sources*, 129 (2004) 264-269
21. X. Xiao, J. Lu and Y. Li, *Nano Research*, 3 (2010) 733-737
22. W. Stöber, A. Fink and E. Bohn, *J. Colloid Interf. Sci.*, 26 (1968) 62-69
23. N. I. Kovtyukhova, T. E. Mallouk and T. S. Mayer, *Adv. Mater.*, 15 (2003) 780-785